Journal of Metals, Materials and Minerals, Vol.29 No.2 pp.27-36, 2019

Corrosion behaviors of ship structural steel in simulated marine tidal environment

Nattapol JAIYOS[1], Ekkarut VIYANIT[2], Pinai MUNGSANTISUK[3], and Kumpanat SIRIVEDIN[1,*]

[1]*The Sirindhorn International Thai-German Graduate School of Engineering (TGGS), KingMongkut,s University of Technology North Bangkok (KMUTNB), Wongsawang, *Bangsue / Bangkok, 10800, Thailand*
[2]*National Metal and Materials Technology Center (MTEC), National Science and Technology Development Agency (NSTDA), Pathumthani, 12120, Thailand*
[3]*Thai Marine Protection, Bangphasi, Bang len, Nakhonprathom, 73130, Thailand*

***Corresponding author e-mail:** kumpanat.s@tggs.kmutnb.ac.th

Received date:
30 September 2018
Revised date:
27 December 2018
Accepted date:
28 December 2018

Keywords:
Marine tidal corrosion
EIS sensor
Corrosion rate
Ship structural steels

Abstract

The tidal zone is severe marine environment for steel structures due to its wet-dry cyclic corrosion pattern. Regarding a specific application for inner ship hull, ship structural steel is always prone to corrosion dealing with three marine environments, including atmospheric, tidal, and immersion zones. Therefore, the current study aimed to investigate corrosion behaviors of two commercial ship structural steels, i.e. alloys A and B, which were exposed to simulated marine tidal environment. The effects of specimen arrangements designated as the isolated short-scale and vertical long-scale specimens were also determined. Based on weight loss determination, it revealed that the corrosion rates of isolated short steel specimens exposed in the tidal zone were almost two times larger than that of vertical long-scale steel specimen. In the tidal zone, the corrosion rates of isolated short-scale steel obtained from weight loss determination quite agreed with the EIS corrosion sensor results. Based on the corrosion resistance aspects, the alloy A is slightly better than the alloy B.

1. Introduction

A tidal zone is recognized as more severe marine environment when compared to the atmospheric and immersion zones. During exposure in the tidal zone, environmental alternation, i.e. wet-dry cyclic pattern, is a considerable factor to accelerate corrosion of steel structure. Tomashov [1] reported that a thickness of electrolyte film formed on the metal surface played a key role in controlling the corrosion rate of metal during exposure to atmospheric environment. The greatest corrosion rate was attributed to the formation of electrolyte film with approximately 10 μm thickness on the metal surface.

Regarding the application of ship in marine environment, the ballast tanks filled up with sea water are normally introduced at various locations of a ship for maintaining the ship's stability during sea voyage. Under an actual service condition, such ballast tanks have to undergo marine tidal environment due to seawater charge/discharge. In general, the paint coating and electrochemical cathodic protection cannot effectively mitigate corrosion of ship steel structure because of high-frequency wet-dry alternation in the tidal zone leading to the damages in coatings. As a result, the steel surface is directly in contact with corrosive electrolyte as reported by Tang et al. [2]. Moreover, the ineffectiveness of cathodic protection is occurred under the wet-dry cyclic pattern due to insufficiency of the ionic return paths through seawater [3]. Therefore, it is very necessary to gain a better understanding on corrosion mechanism of ship structural steel under marine tidal environment in order to select an appropriate means of corrosion mitigation.

As reported in the previous literatures [4,5], the formation of macroscopic corrosion could slow down the corrosion rate of the vertical long-scale carbon steel with respect to the short isolated carbon steel exposed in the tidal zone. In contrast, the higher corrosion rates were obtained for the vertical long scale specimen compared with the short isolated specimen when exposed in the immersion zone.

According to ASTM-A131 [6], an ordinary structural steel with normal strength (yield strength ≈ 235 MPa) represented by alloy A is normally used in shipbuilding. On the other hand, a higher strength

DOI: 10.14456/jmmm.2019.15

steel, alloy B, is recommended for building a ship which requires special characteristics such as bulk carriers, containers, etc. However, corrosion behavior of those steels exposed in marine tidal environment is widely discussed. Therefore, the current study aims to investigate the corrosion behaviors of alloys A and B in a simulated marine tidal zone by means of weight loss calculation and EIS-sensor corrosion monitoring. In addition, two arrangements of testing steel specimens, i.e. isolated short-scale and vertical long-scale specimens, were also included as a key factor to influence the corrosion behavior of steel specimens.

2. Experimental

2.1 Specimen preparation

2.1.1 Steel specimens

The rectangular test specimens with a dimension of 70 mm × 70 mm × 5 mm were prepared from two commercial ship structural steels, alloys A and B, whose chemical compositions are given in Table 1. Hot-rolled oxide scales present on the steel surface were removed by using sand blasting, Sa2½, in accordance to ISO 8501-1:88 [7]. The freshly descaled steel specimens were then selectively wrapped by adhesive tape in order to prevent the formation of atmospheric corrosion products and to confine an exposure area of 50 mm × 50 mm for corrosion testing. Epoxy-based paint coating was applied to eliminate any sensitive area which will be able to interfere the accuracy of corrosion testing results as shown in Figure 1(a). Regarding the formation of vertical long scale specimen, an insulated lead wires were used for electrical connectivity to compose a series of the isolated short scale specimens as shown in Figure 1(b).

2.1.2 EIS sensors

In order to monitor the corrosion behavior of ship structural steels, a comb-shaped EIS corrosion sensor consisting of two identical-dimension electrodes (see Figure 2) was made of the given steel. Prior to exposure in the simulated marine tidal environment, the EIS corrosion sensors were ground using emery paper down to 2000 grit, rinsed with acetone, and dried off by compressed hot air. The EIS corrosion sensors were vertically allocated to acquire corrosion behavior of the steel in the various positions representing the environmental conditions of atmospheric and tidal zones (see Figure 3). In the atmospheric zone, two EIS corrosion sensors designated as sensors A and B were installed at 4 and 24 cm far from the high water level (HWL). In the tidal zone, the positions for installation of EIS corrosion sensors were 4, 14, and 34 cm below the HWL, which were designated as C, D, and E, respectively. EIS measurement was conducted over a frequency range from 100 kHz to 10 mHz with the peak-to-peak amplitude of 10 mV using a potentiostat/galvanostat (AUTOLAB PGSTAT302N).

Table 1. Chemical compositions of ship structural steels used in the current study.

Steels	C	Si	Mn	P	S	Cr	Ti	Nb	Cu	Fe
Alloy A	0.065	0.041	0.772	0.005	0.001	0.007	0.001	0.017	0.044	Bal.
Alloy B	0.137	0.393	1.428	0.014	0.002	0.035	0.001	0.001	0.010	Bal.

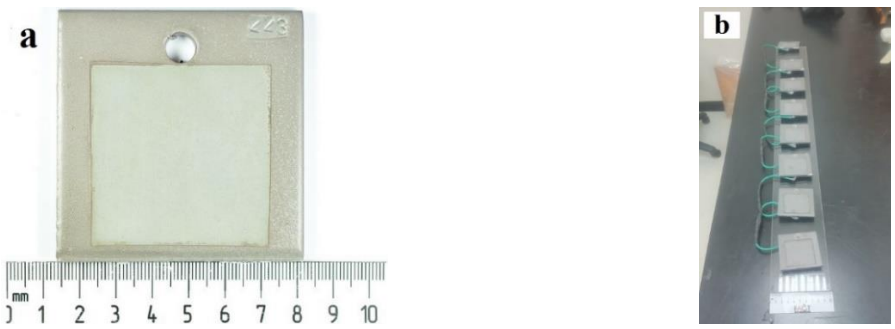

Figure 1. Preparation of corrosion test specimens : (a) isoleted short scale and (b) vertical long scale.

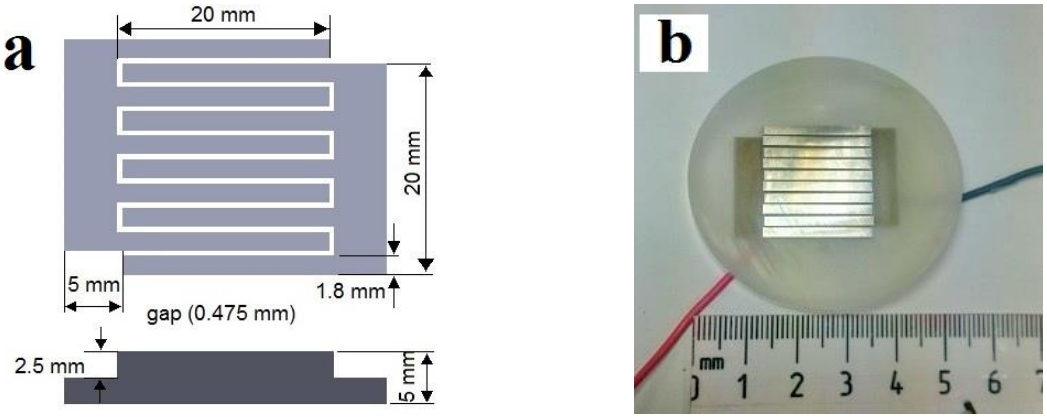

Figure 2. EIS corrosion sensor: (a) EIS sensor dimensions and (b) top view of EIS sensor before experiment.

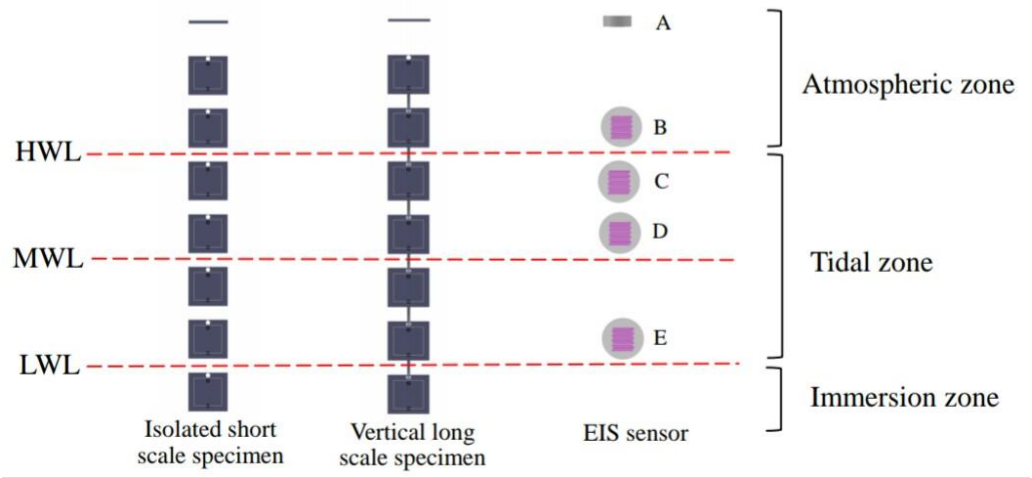

Figure 3. Schematic diagram of simulated tidal marine experiment.

Table 2. Synthetic seawater with chemical composition.

Compound	Concentration g/90L
NaCl	2207.7
Na_2SO_4	368.1
KCl	62.55
$NaHCO_3$	18.09
KBr	9.09
H_3BO_3	2.43
NaF	0.27
$MgCl_2.6H_2O$	998.91
$SrCl_2.6H_2O$	3.78
$CaCl_2.2H_2O$	138.33

2.2 Marine tidal corrosion simulation

A marine tidal corrosion simulator was used to investigate the corrosion behaviors of the ship structural steels with taking into account the environmental parameters in the atmospheric, tidal and immersion zones. The tidal zone was defined in between 13 cm (lower water level: LWL) and 53 cm (HWL) of water height as schematically shown in Figure 3. The immersion and atmospheric zones were specified at the water height below 13 cm and above 53 cm, respectively. The testing solution was synthetic seawater whose chemical composition is shown in Table 2.

In order to simulate the marine tidal zone representing the actual service condition in a ballast tank of the ship, the seawater level was periodically alternated between the low and high tides. The holding period at the low and high water levels was 356 min. Both water ramp-up and ramp-down cycles were completely done in 4 min. Figure 4 shows a cyclic pattern for corrosion testing in marine tidal environment. One complete tidal cycle took 12 h. In the current study, the tidal alternation of 120 cycles was set for experimental completion. After that the corrosion behavior of the exposed specimens was determined based on weight loss measurement compared with EIS results. Descaling of the exposed steel specimens was conducted in accordance to ASTM G1-99 [8].

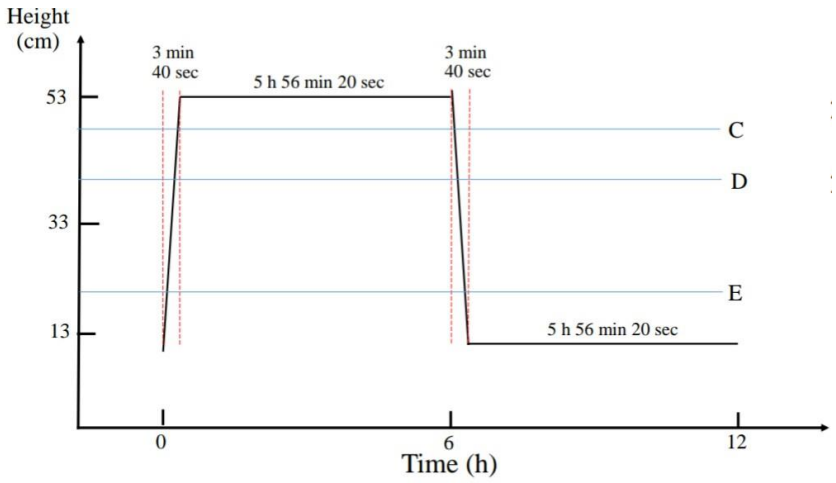

Figure 4. The tidal curve in a cycle.

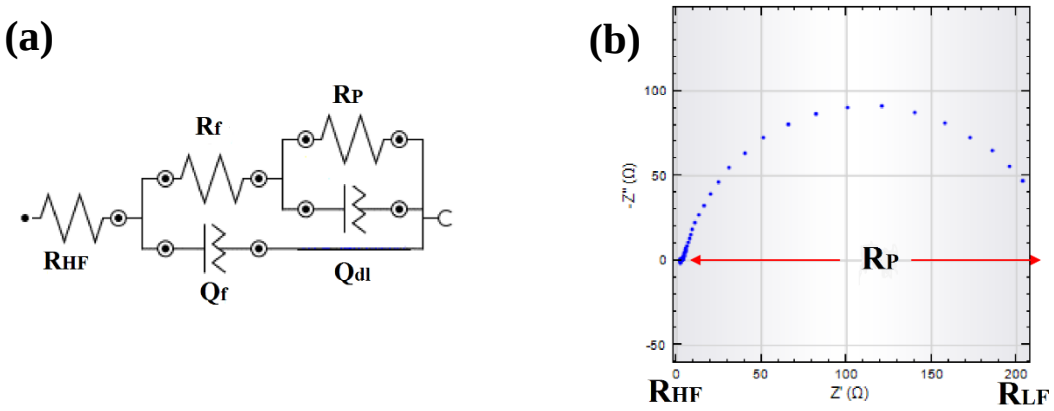

Figure 5. (a) Equivalent circuit of electrode/electrolyte and (b) nyquist plot of EIS.

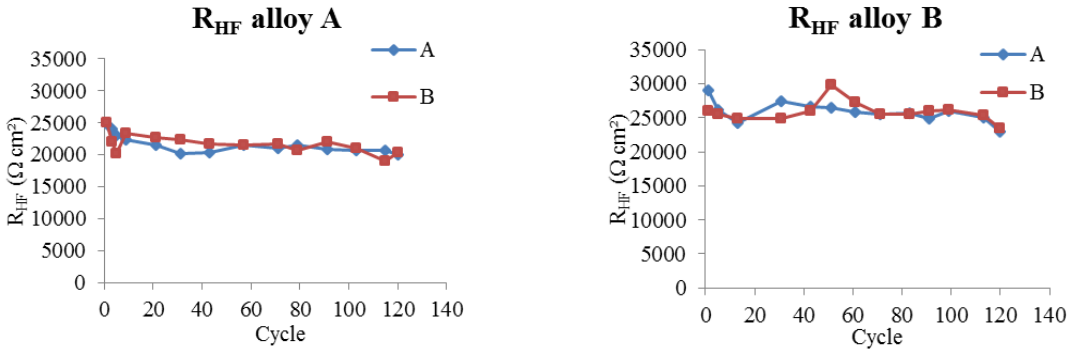

Figure 6. Correlation between a number of tidal cycles and R_{HF} acquire from EIS corrosion sensors exposed in the atmospheric zone.

3. Results and discussion

3.1 EIS corrosion sensor

Based on EIS principle according to ASTM G3 [9], the corrosion behavior of steel exposed to electrolyte can be described by an equivalent circuit (EC) as shown in Figure 5. High-frequency resistance (R_{HF}) represents the sum of solution resistance (R_s) and rust resistance (R_r). The resistance and capacitance of rust layer are denoted by R_f and Q_f, respectively. Q_{dl} and R_P are used to describe the double layer capacitance and polarization resistance, respectively.

In the previous studies [4,5,10], they suggested that the solution resistance (R_s) can be represented

by R_{HF} at a frequency of 100 kHz. In the immersion state, R_{HF} becomes small and stable due to the sufficient electrical conductivity caused by seawater. However, R_{HF} is increased as a thickness of electrolyte film on the steel surface decreased. Based on the suggestions by some researchers [4,10,11], a completely dry state could be assumed when R_{HF} was larger than 1,000 Ω·cm^2. Figure 6 clearly reveals that the atmospheric zone cannot significantly cause corrosion to occur in both alloys A and B because the R_{HF} values acquired from EIS sensors are above 20,000 Ω·cm^2 which is categorized into a dry state. Figure 7 shows the R_{HF} values obtained from the different EIS corrosion sensors, sensors C, D and E, in the marine tidal zone. In overall, it can be seen that the highest R_{HF} values are revealed in the early tidal cycles, which tend to decrease as the number of tidal cycles increased. At the given number of tidal cycles, the R_{HF} values are abruptly dropped when electrolyte reached to the EIS sensor during an immersion stage. It is quite interesting for R_{HF} values in the first tidal, for example, the R_{HF} value starts at around 70 Ω.cm² and gradually increased to 130 Ω.cm² as a time of exposure period in the dry stage (ebb tide) increased. As the sensor exposed to electrolyte in the immersion state (flood tide), the R_{HF} value abruptly dropped to 4 Ω.cm² and remained until the beginning of dry stage. From this, it can be said that an increase in corrosion product thickness, a high quantity of electrolyte can remain in the corrosion product, resulting no obvious variation of the R_{HF} values even in the dry state. This finding is clearly noticed for all the sensors installed in the tidal zone when the tidal cycles of 120 were reached. Figure 8 shows a ratio between the immersion and wet periods of time calculated based on electrochemical aspects form the sensors C, D, and E. It is seen that the duration of immersion state found in the sensor C is slightly smaller than those of the sensors D and E. The largest duration of immersion state is obtained for the sensor E. This can explain why the sensor E indicates its lowest R_{HF} values with respect to the other sensors.

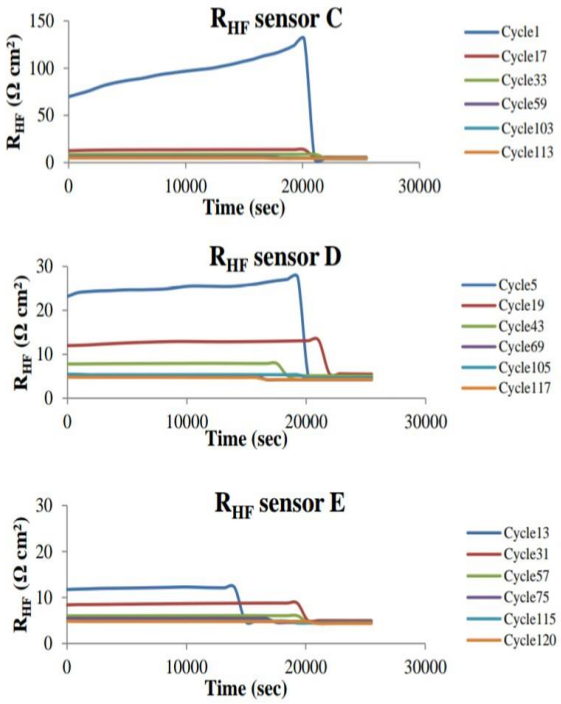

Figure 7. Correlation between a number of tidal cycles and R_{HF} in tidal zone.

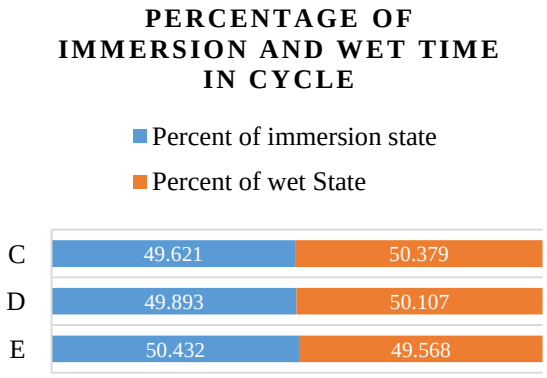

Figure 8. Percentage of immersion and wet time in cycle.

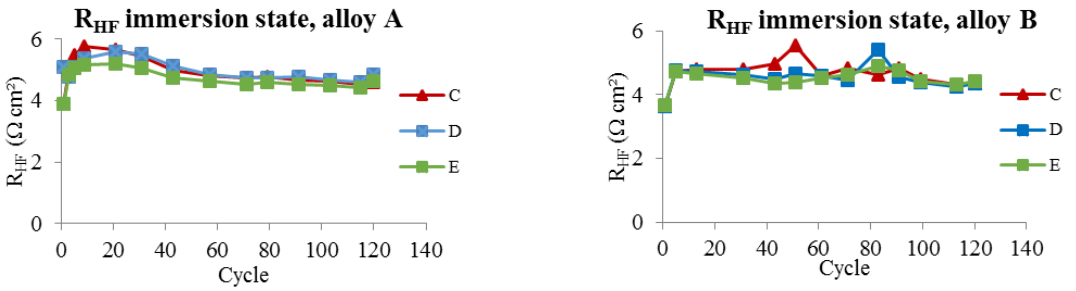

Figure 9. Correlation between a number of tidal cycles and R_{HF} acquired from EIS corrosion sensors exposed in the tidal zone during an immersion state.

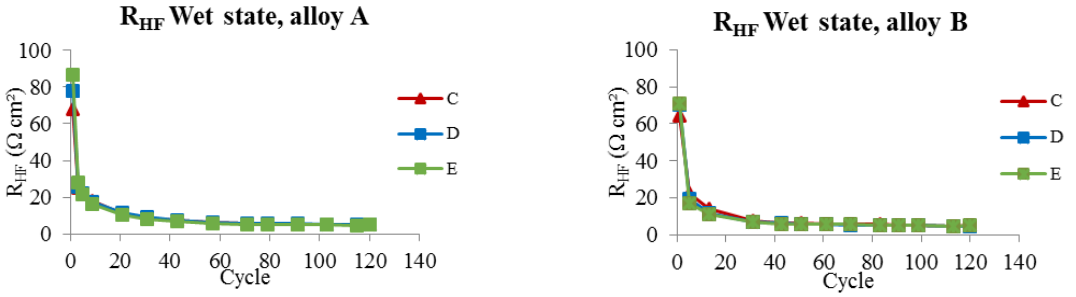

Figure 10. Correlation between a number of tidal cycles and R_{HF} acquired from EIS corrosion sensors exposed in the tidal zone during a wet state.

Based on the R_{HF} point of view, the environmental factors in the marine tidal zone can cause much more severe corrosion attack of carbon steel when compared with the marine atmospheric zone. The R_{HF} values of the alloys A and B exposed in the marine tidal zone during the immersion and wet states are shown in Figure 9 and 10, respectively. In the immersion state, both alloys A and B reveal their R_{HF} values in a range between 4 and 6 $\Omega \cdot cm^2$. Increasing the number of tidal cycles could not obviously affect the variation of R_{HF} values due to a direct contact of the steel samples to bulk seawater (electrolyte solution). It is worth to note that the lowered R_{HF} values during the early tidal cycles should refer to the small quantity of corrosion products formed on the steel surface, promoting the migration of ions in the solution to occur easily. On the other hand, an increase in the R_{HF} values should be attributed to compactness characteristic of the corrosion product which impair the mobility of ions transfer between the steel surface and electrolyte [3]. As the sufficient number of tidal cycles was achieved, the protective property of corrosion product was loosen due to their volumetric enlargement, leading to a decrease of R_{HF} values. In the wet state (Figure 10), the R_{HF} values abruptly drop as the number of tidal increased, in particular during the tidal cycles of 1 to 5. Afterwards, the R_{HF} values gradually decrease with increasing the number of tidal cycles. Regarding the much higher R_{HF} values in the wet state with respect to the immersion state during the early state of exposure (cycle 1 to cycle 5), it is attributed to insufficiency of electrolyte film formed the steel surface, leading to an increase in impedance between two sensor electrodes. However, it is worth to note that the R_{HF} values obtained in the immersion state are almost similar to those obtained in the wet state after a tidal cycle 20 is exceeded. It reveals that the sufficient quantity of corrosion products formed on the steel surface could maintain the electrolyte as long as the next cycle of immersion started again.

Figure 11 shows the R_P^{-1} values a function of the number of tidal cycles, which were acquired from the sensors C, D, and E made of the alloys A and B. In the early cycles of immersion state, the R_P^{-1} values increases rapidly until a 40th cycle. After that, the R_P^{-1} values changed not much as the number of tidal cycles increased, because the compacted corrosion products obstructed oxygen diffusion from the electrolyte to the metal surface. However, R_P^{-1} of steel exposed in the wet state becomes more stable than the immersion state as shown in Figure 12 from two reasons, on the one hand, with the increase of cycles, the thickening and compactness of the rust layer obstruct oxygen migration to the steel substrate and as the result in decrease R_P^{-1}. On the other hand, the liquid film thickness and seawater content on steel surface also increase with the increase of rust thickness, which leads to the higher ions conducting ability and thus increase R_P^{-1}. Therefore, the combined of two effects result in the stable $R_P^{-1}$with the increase of cycles.

Comparing between the alloy A and the alloy B, their R_P^{-1} values are almost similar. Regarding to the wet state as shown in Figure 12, the R_P^{-1} values of both alloys are not significantly varied as the number of tidal cycles increased. The explanation for those phenomena should refer to an increase in thickness and compactness of the corrosion products that obstructed oxygen migration from the electrolyte to the steel substrate. On the other hand, the thickness of the electrolyte film on the alloy surface increases as the corrosion products become thicker, resulting in an increase of the R_P^{-1}values. However, it is worth to note that the R_P^{-1}values obtained for the alloy B is higher than those of the alloy A. It should be attributed to the fact the alloy B is to be polarized more easily with respect to the alloy A.

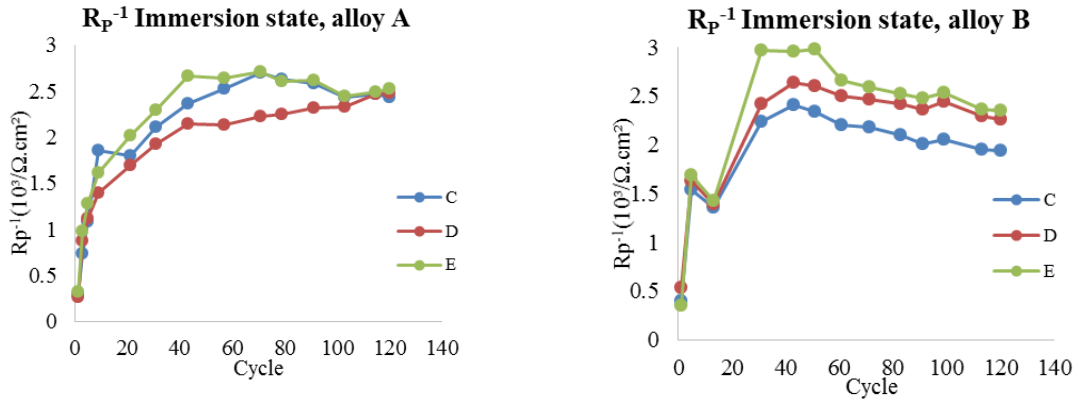

Figure 11. Correlation between a number of tidal cycles and reciprocal polarization resistance (R_P^{-1}) acquired from EIS corrosion sensors exposed in the tidal zone during a immersion state.

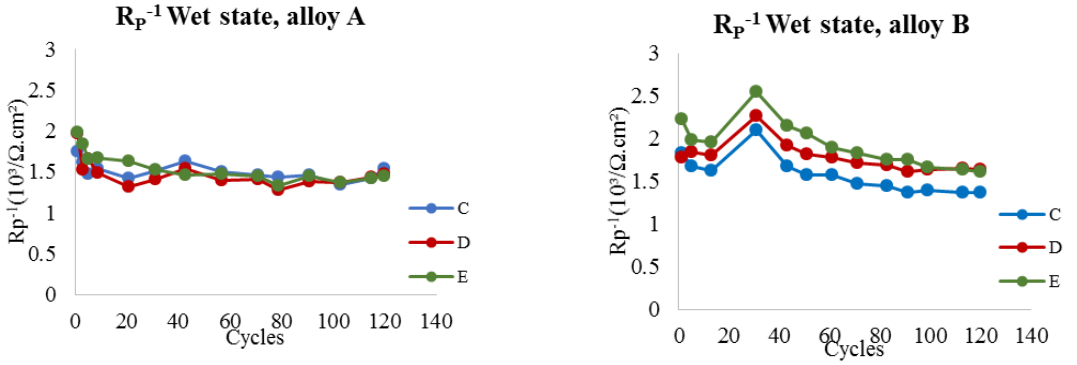

Figure 12. Correlation between a number of tidal cycles and reciprocal polarization resistance (R_P^{-1}) acquired from EIS corrosion sensors exposed in the tidal zone during a wet state.

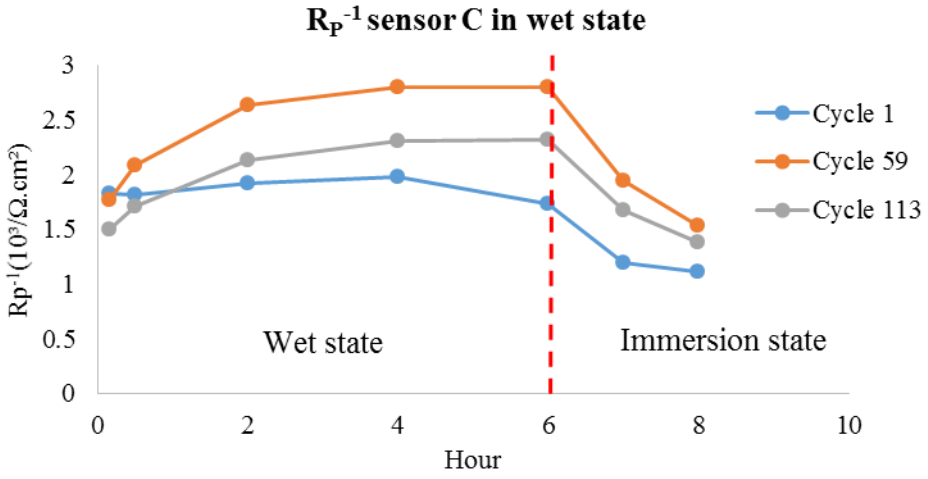

Figure 13. The reciprocal polarization resistance (R_P^{-1}) at the tidal cycles of 1, 59 and 113 during exposure to the wet and immersion states of the tidal zone.

Figure 13 shows the R_P^{-1} values obtained from the sensor C made of the alloy B during exposure in the marine tidal zone at the 1st, 59th, and 113rd tidal cycles. In the first cycle, the R_P^{-1} values gradually increase until the exposure duration of 4 h in the wet state is exceeded and then slowly decrease until the beginning of immersion state because of the less quantity of corrosion products formed on the exposed surface of the alloy. As the number of tidal cycles increase, i.e. 59th and 113rd cycles, the R_P^{-1}

values are increased. But, the R_P^{-1} values obtained from 59th cycle are relatively higher than those obtained from the 113rd cycle. This finding should be attributed to the characteristics of corrosion products which are not so compacted when the thickness of corrosion product increased. In addition, it is clearly seen that the R_P^{-1} values of the alloy exposed to the immersion state are lower than those exposed in the wet state, indicating that the corrosion in the wet state are more severe than the immersion state.

3.2 Corrosion weight loss

Figure 14 shows the corrosion rate of alloy B in correlation with the specimen arrangements, i.e. isolated short and vertical long scale specimens, after being exposed in the simulated marine tidal environment with 120 cycles. The corrosion rate was determined based on a weight loss basis. It clearly reveals that the corrosion rates of the alloys exposed in simulated marine tidal environment are in an order from high to low: tidal zone > immersion zone > atmospheric zone. In comparison between the isolated short specimens and the vertical long scale specimens, their corrosion rates in the tidal zone exhibit a difference in corrosion behavior. The corrosion rates of the isolated short scale specimens are obviously higher than those of the vertical long scale specimens. An average corrosion rate is 0.50 $mm \cdot y^{-1}$ for the isolated short scale specimens whereas the vertical long scale specimens exhibit an average corrosion rate of 0.30 $mm \cdot y^{-1}$. In immersion and atmospheric zone, the corrosion rates of the vertical long scale specimens are higher than those of the isolated short scale specimens.

The corrosion rates of isolated short scale specimens exposed in the marine tidal zone are around 5 times larger than those exposed in the immersion zone, and more than 14 times exposed in the atmospheric zone. It means that the environmental parameters of marine tidal zone can significantly accelerate corrosion attack due to its immersion-wet-dry cyclic characteristics, especially oxygen transport through the electrolyte film can occur in the wet state more easily. The oxygen transport rate dominates the rates of cathodic reaction of metallic corrosion. The thinner the film is, the faster the oxygen transports to the metal surface, and the higher the cathodic reaction rate is. In addition, a change in the concentration of existing anion Cl^- and probably a change in the pH of electrolyte can occur under an influence of a change in thickness of the electrolyte film [1,4,11-13].

In the tidal zone, the corrosion rates of the vertical long scale specimens are lower than those of the isolated short scale specimens because of the formation of the macroscopic corrosion cell between the tidal zone and the immersion zone. The electrically connected specimens in the tidal zone serve as the cathode of the corrosion cell which can receive electrons produced through corrosion of the alloy exposed in the immersion zone. In contrast, there is no a macroscopic corrosion cell formed in the isolated short scale specimens [4,5,13].

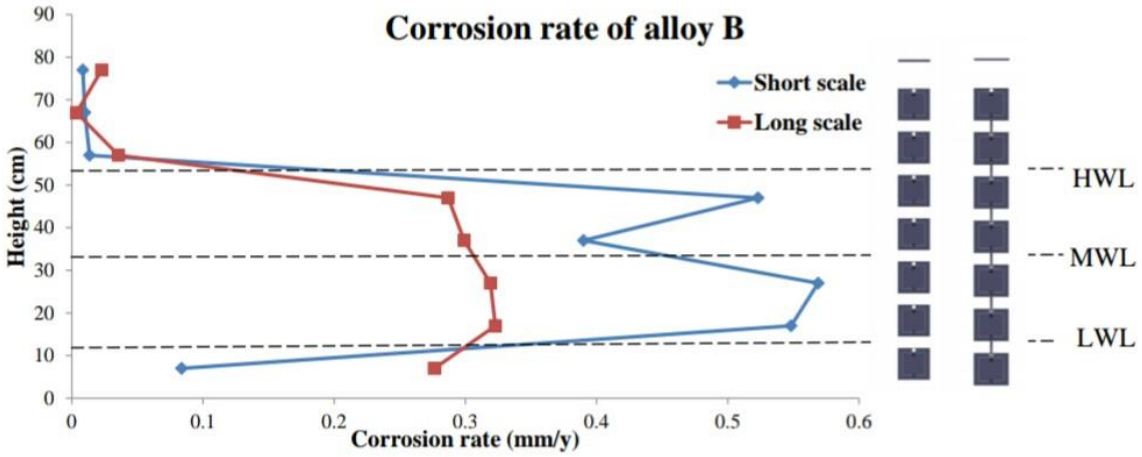

Figure 14. Corrosion rate of isolated short-scale and vertical long-scale alloy B specimens after completion of 120-cycle tidal marine corrosion simulation.

3.4 Calculation of corrosion rate from EIS sensor

The corrosion rate was calculated by Eq. (1) according to ASTM G102-99 [14].

$$CR = k_1 \frac{i_{corr}}{\rho} EW \quad (1)$$

Where CR ($mm \cdot y^{-1}$) represents the average corrosion rate, k_1 (3.27×10^{-3} mm g·μA^{-1}·cm^{-1}·yr^{-1}), ρ (7.86 g·cm^{-3}) the density of iron, EW (27.92) equivalent weight of iron, i_{corr} (μA·cm^{-2}) the corrosion current density, i_{corr} is calculated by Eq. (2),

$$i_{corr} = k \frac{\sum_N (R^{-1}_{p(immersion)} t_{immersion} + R^{-1}_{p(wet)} t_{wet})}{\sum_N (t_{immersion} + t_{wet})} \quad (2)$$

Where the Eq.(2) according to Xin Mu et al. [4], R_P^{-1} is the polarization resistance acquired from Figure 11 and 12, $t_{immersion}$ and t_{wet} are the immersion and wet time in a cycle obtained from the results of Figure 8, respectively, k is the Stern-Geary constant with the value of 0.025 V [15], N is the number of corrosion cycles ranging from 0 to 120.

Figure 15 shows the corrosion rates acquired from EIS sensors results compared with those calculated based on weight loss measurement of the alloys A and B installed at the different positions in the marine tidal zone. Based on both EIS sensor and weight loss measurement corrosion rate calculation, the alloy A exhibits the corrosion resistance better than the alloy B approximately 0.1 $mm \cdot y^{-1}$. The corrosion rate results calculated from the EIS sensor quite agree with those calculated based on weight loss measurement of the exposed specimens. Therefore, the applications of EIS sensors are feasible for corrosion monitoring of steel components and structures that have to be exposed in the marine tidal environment.

4. Conclusions

1) The corrosiveness of simulated marine tidal environment for ship structural steel can be ranked from high to low: Tidal zone > Immersion zone > Atmospheric zone.
2) Corrosion rate of vertical long-scale steel is lower than that of isolated short-scale steel during exposure in the tidal zone, but higher during exposure in the immersion zone because of the formation of macroscopic corrosion cell supplying electrons for corrosion protection in the tidal zone.
3) Application of EIS sensor for corrosion monitoring is suitable for both immersion and wet states of the tidal zone.
4) Corrosion rate results of ship structural steel obtained from weight loss determination quite agree with that obtained from EIS corrosion sensors.
5) In simulated marine tidal environment, the alloy A reveals better corrosion resistance than the alloy B.

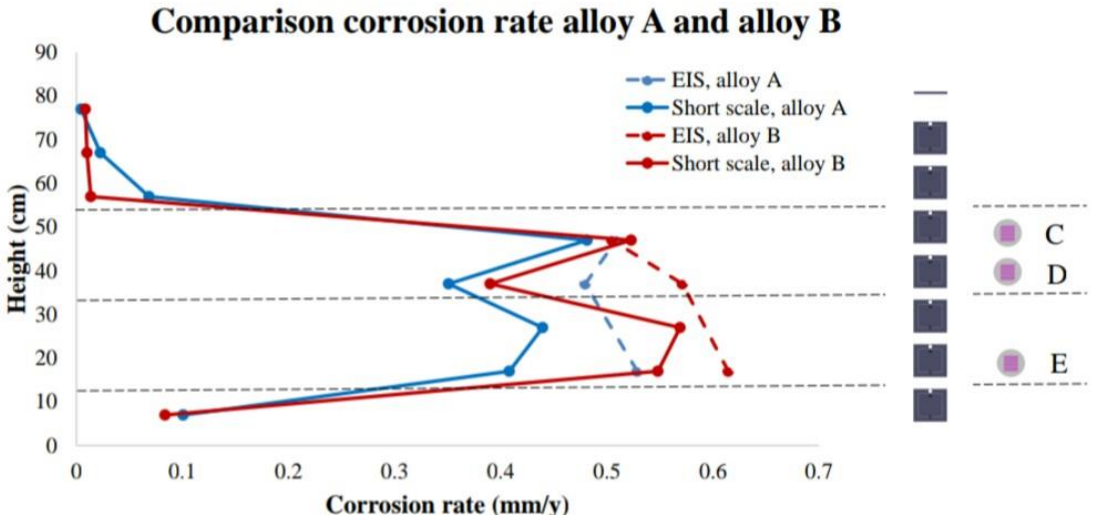

Figure 15. Comparison of corrosion rates obtained from weight loss determination and EIS corrosion sensor calculation for alloys A and B.

5. Acknowledgements

This project was financially supported by Royal Thai Naval Dockyard. The authors are grateful to technical support provided by National Metal and Materials Technology Center (MTEC), Thailand.

References

[1] N. D. Tomashov, "Development of the electrochemical theory of metallic corrosion," *Corrosion*, vol. 20, pp. 7-14, 1964.

[2] Y. Tang, J. Cao, S. Qu, L. Quan, X. Zhao, and Y. Zuo "Degradation of a high build epoxy primer/polyurethane composite coatings under cyclic wet–dry conditions," *International Journal of Electrochemical Science*, vol. 13, pp. 3874 – 3887, 2018.

[3] E. Bardal, *Corrosion and Protection*. London: Springer-Verlag London Limited, 2003.

[4] M. Xin, W. Jie, D. Junhua, and K. Wei, "In situ corrosion monitoring of mild steel in a simulated tidal zone without marine fouling attachment by electrochemical impedance spectroscopy," *Journal of Materials Science & Technology*, vol. 30, pp. 1043-1050, 2014.

[5] B. R. Hou, J. L. Zhang, H. Y. Sun, Y. Li, and B. Xiang, "Corrosion of C–Mn steel in simulated tidal and immersion zones," *British Corrosion Journal*, vol. 36, pp. 310-312, 2001.

[6] ASTM A131, Standard Specification for Structural Steel for Ships, The American Society for Testing and Material, 2004.

[7] ISO 8501-1, Rust grades and preparation of uncoated steel substrates and steel substrates after overall removal of previous coatings, International Organization for Standardization, 2007.

[8] ASTM G1, Standard Practice for Preparing, Cleaning, and Evaluating Corrosion Test Specimens, The American Society for Testing and Materials, 1999.

[9] ASTM G3, Standard Practice for Conventions Applicable to Electrochemical Measurementsin Corrosion Testing, The American Society for Testing and Material, 1999.

[10] A. P. Yadav, A. Nishikata, and T. Tsuru, "Electrochemical impedance study on galvanized steel corrosion under cyclic wet–dryconditions-influence of time of wetness," *Corrosion Science*, vol. 46, pp. 169-181, 2004.

[11] X. X. Fu, J. H. Dong, E. H. Han, and W. Ke, "A new experimental method for in situ corrosion monitoring under alternate wet-dry conditions," *Sensors (Basel)*, vol. 9, pp. 10400-10410, 2009.

[12] A. Nishikata, Y. Ichihara, and T. Tsuru, "An appriction of electrochemical impedance spectroscopy to atmospheric corrosion study," *Corrosion Science*, vol. 37, pp. 897-911, 1995.

[13] R. Jeffrey and R. E. Melchers, "Effect of vertical length on corrosion of steel in the tidal zone," *Corrosion*, vol. 65, pp. 695-702, 2009.

[14] ASTM G102, Standard Practice for Calculation of Corrosion Rates and Related Information from Electrochemical Measurements, The American Society for Testing and Materials, 1999.

[15] T. Tsuru, S. Haruyama, and B. Gijutu, "Corrosion monitor based on impedance method; construction and its application to homogeneous corrosion," *Japan Society of Corrosion Engineering*, vol. 27, pp. 573-579, 1978.